Biochimica et Biophysica Acta, 979 (1989) 82–90
Elsevier

BBA 74319

Thermodynamic and kinetic studies on the association of melittin with a phospholipid bilayer

Gerhard Schwarz and Georgi Beschiaschvili

Department of Biophysical Chemistry, Biocenter of the University of Basel, Basel (Switzerland)

(Received 8 August 1988)
(Revised manuscript received 7 November 1988)

Key words: Melittin; Phospholipid bilayer; Protein–membrane interaction; Kinetics; Thermodynamics

Association of the amphiphilic peptide melittin with unilamellar vesicles of dioleoylphosphatidylcholine has been experimentally investigated by means of circular dichroism, fluorescence energy transfer and stopped-flow experiments. Circular dichroism changes upon titration of the peptide with vesicles (at low salt concentration) were analyzed to yield thermodynamic association isotherms. These isotherms are quantitatively interpreted in terms of a monomer-monomer partitioning of melittin between the aqueous and bilayer media. The data can be very well fitted by theoretical curves based on a Gouy-Chapman surface potential. Energy transfer involving chemically modified tryptophan confirms a lack of aggregation of the associated peptide. According to the kinetic measurements the association proceeds in practice as a one-step process, which is rather fast but not fully diffusion-controlled. We propose a simple mechanism where the inherent conformational transition determines the overall rate.

Introduction

Melittin, the main constituent of bee venom, is a peptide of 26 amino-acid residues ($M_r = 2840$) [1]. The 20 residues on the N-terminal side are largely hydrophobic, whereas the other 6 at the C-terminus are polar. Owing to its amphipathic nature, melittin is easily soluble in aqueous media, but also associates strongly with detergents and phospholipid bilayers [2]. These features have made melittin a popular model with which to investigate protein–membrane interactions.

Upon association with a membrane, at least some of the hydrophobic part of the peptide penetrates the apolar moiety of the lipid molecules. Greater or lesser insertion in the core of the bilayer can be inferred from spectroscopic data [3,4], voltage-dependent pore formation [5], lytic effects [6] and lipid monolayer experiments [7].

We consider the apparent incorporation mode of association inappropriate for a quantitative discussion in terms of a binding process. There is no indication of clearly defined binding sites, which would be saturated at high peptide/lipid concentrations. Instead, the lipid bilayer must be seen to function as a two-dimensional solvent. This implies favorable solvation effects of the lipid towards the peptide. Accordingly, we prefer to describe the association on the basis of a partitioning of melittin between aqueous and lipid phases. Such an approach has been accomplished recently for another membrane active substance, the antibiotic peptide alamethicin [8–10].

In the present article we report on analogous work with melittin and unilamellar vesicles made of DOPC. Circular-dichroism changes upon titration and transient fluorescence signals after rapid mixing are evaluated to give quantitative information about the extent and the kinetics of the association process, respectively. In addition, the aggregational state of the associated peptide is probed by means of fluorescence energy transfer measurements.

Our results provide insight into the basic physical chemistry of melittin interactions with a lipid bilayer in the fluid state. Under the given conditions, a rather simple quantitative picture can be established. The peptide 'dissolves' as a monomer in the lipid moiety, where electrostatic solute–solute repulsion gives rise to thermodynamically non-ideal effects. Melittin molecules from the outside may enter the bilayer by diffusion and then undergo a rate-limiting change of secondary struc-

Abbreviations: DOPC, 1,2-dioleoylphosphatidylcholine; DMPC, dimyristoylphosphatidylcholine; PBA, 1-pyrenebutyric acid.

Correspondence: G. Schwarz, Abteilung für Biophysikalische Chemie, Biozentrum der Universität, Klingelbergstrasse 70, CH-4056 Basel, Switzerland.

ture. The average lifetime inside the bilayer is of the order of 100 ms.

Materials and Methods

Melittin was purchased from Mack Chemical (Illertissen, F.R.G.). In order to remove possible remnants of phospholipase A_2 ($M_r \approx 19000$ [11]) an aqueous solution of the originally brown material (approx. 10 mg/ml) was purified by pressure filtration using Diaflo YM 10 membranes only permeable to molecules having an M_r below about 10000. After freeze-drying, we obtained a white cotton-like substance. Having incubated this purified melittin for 1 day with a dispersion of DMPC, thin-layer chromatography indicated no sign of decomposition products. Moreover, we always added 1 mM EDTA to the buffer used in the association experiments. This would fully inactivate the enzyme by removing the Ca^{2+} in the active site [11]. Electrophoresis of the purified material showed, aside from the main peptide component, only a trace of the formylated species (less than 5%). This is expected not to impair our experiments to any significant degree. The peptide concentration was determined from ultraviolet absorption recorded on a Varian Techtron 634, applying a molar optical absorption coefficient of 5570 $M^{-1} \cdot cm^{-1}$ at 280 nm [12].

Some of the melittin was chemically modified by reaction of its Trp residue with 2-hydroxy-5-nitrobenzyl bromide (from Serva, Heidelberg, F.R.G.). For details see Ref. 13.

Unilamellar vesicles of DOPC from Avanti Polar Lipids (Birmingham, AL, U.S.A.) were prepared as follows. A lipid dispersion (approx. 3 mg/ml) in buffer (10 mM Tris-HCl (pH 7.1)/1 mM EDTA) was sonicated under a nitrogen atmosphere for 40 min (at 10 °C). Metal debris from the titanium tip was removed by centrifugation.

Fluorescence spectra were recorded with a Schoeffel RRS 1000 spectrofluorometer (excitation at 280 nm with 2 nm bandwidth, emission of unmodified Trp in the range of 300–400 nm with 3.5 nm bandwidth).

The circular-dichroism measurements were performed with a Cary 61 instrument, which had been calibrated using D(+)-10-camphor sulfonic acid.

The kinetic measurements were done in a thermostatically controlled Durrum stopped-flow apparatus (dead-time, 2.8 ms) with two monochromators and a fluorescence detection system as developed in this department [14]. The fluorescence was excited at 282 nm (7 nm bandwidth). All the solutions were carefully degassed.

In our experiments we always maintained a temperature of 18 °C and a pH of 7.1 (10 mM Tris-HCl), except for the fluorescence energy transfer study, where the pH was 5 (using 10 mM phosphate buffer). Inner filter effects in the fluorescence measurements became negligible because of the low melittin concentration.

Results

Association isotherms

At concentrations below approx. 0.1 mM, at neutral pH and with a little extra electrolyte added, melittin in aqueous solution exists as monomeric molecules with a low degree of secondary structure [12,15]. Accordingly, it exhibits a comparatively weak circular-dichroism spectrum around 220 nm. This spectrum becomes more and more pronounced, however, if unilamellar lipid vesicle preparations are added [16]. The effect is apparently caused by an increase of helical structure when the peptide somehow associates with the lipid bilayer. Changes of the circular-dichroism signal depending on the total lipid-to-peptide ratio can therefore be used to determine quantitatively the relevant association isotherm, i.e., the amount of associated peptide per lipid as a function of the free aqueous peptide concentration [8,9].

In the present work, a fresh solution was prepared for each data point. Equal volumes of appropriate lipid vesicle and melittin concentrations were mixed a few minutes before the measurement. No kinetic effects could be observed under these circumstances. In order to avoid interference by scattered light we used cuvettes of different optical pathlengths depending on the vesicle concentration. So we determined $\phi = -[\theta]^{225}_{222}$, i.e., the negative ellipticity per residue at 222 nm. The value, ϕ_0, for a lipid-free solution is then subtracted, resulting in $F = \phi - \phi_0$, which is a measure of the fraction of associated peptide. Naturally there is an upper boundary value, F_∞, corresponding to the case where all the peptide is in the associated state. This implies that

$$F = F_\infty \cdot r \cdot (c_L/c_P) \tag{1}$$

where r stands for the associated peptide-to-lipid ratio and c_L and c_P are the total lipid and peptide concentrations, respectively.

We have plotted experimental values of F vs. c_L/c_P at fixed c_P (see for example, Fig. 1). If F_∞ is known, r can readily be calculated by means of Eqn. 1. Subsequently, the relation of mass conservation

$$c_P = r \cdot c_L + c_f \tag{2}$$

is used to determine c_f, the free aqueous peptide concentration.

The quantity F_∞ may be concentration dependent. However, the values of F_∞, r and c_f can be shown to be constant under conditions where $Q = F \cdot (c_P/c_L)$ is conserved. In the diagram of Fig. 1, this applies to straight lines through the origin. Any such straight line may

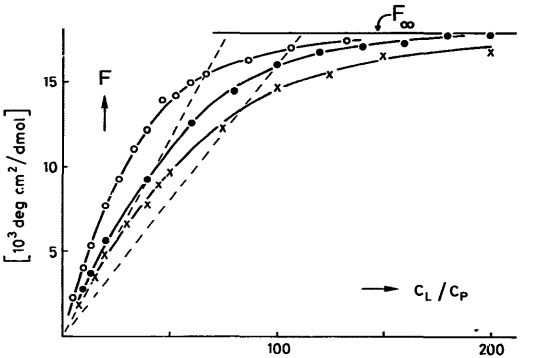

Fig. 1. Increase of negative ellipticity per residue of total melittin at 222 nm, F, vs. the overall lipid-to-peptide ratio. The data have been obtained at 18°C (pH 7.1) (10 mM Tris-HCl/1 mM EDTA) with no extra salt for three melittin concentrations: c_P (μM) = 2 (×), 5 (●) and 15 (○). On straight lines through the origin, $Q = F \cdot c_P / c_L$ is constant. This implies constant values of r and c_f (see text). The examples given (dashed) refer to $Q = 231$ and 160 deg·cm^2·dmol^{-1}, respectively. The quantity F_∞ stands for the ellipticity increase per residue of associated melittin.

intersect two or more experimental curves. The respective c_P and c_L must then be linearly related to each other according to Eqn. 2 with common values of r and c_f [10]. For the system of Fig. 1 (no extra salt added) we have executed this procedure with up to four curves (including also data for $c_P = 20$ μM, which are not presented in Fig. 1), covering values of Q between about 130 and 220 deg · cm^2 · dmol^{-1}. The value of r so

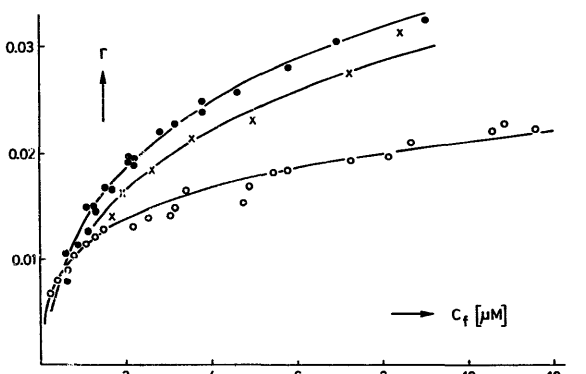

Fig. 2. Association isotherms, r (i.e., associated melittin per lipid) vs. the concentration of free aqueous peptide, c_f. The three sets of data points refer to the same temperature and buffer condition as in Fig. 1, but different concentrations of added NaCl: 0 M (○), 0.1 M (×) and 0.22 M (●). The solid curves have been calculated with Eqns. 6 and 7 as discussed in the text. These fits involve the following values of the parameters ν and Γ_1 (in 10^4 M^{-1}): 1.8/15 (no salt), 1.85/3.0 (0.1 M NaCl) and 2.05/3.2 (0.22 M NaCl). Uncertainties are estimated to be about ±5% for ν and ±20% for Γ_1.

determined led to a practically constant $F_\infty = 18000$ ($\pm 3\%$) deg · cm^2 · dmol^{-1} when Eqn. 1 was applied. This F_∞ has been used to calculate r and c_f also under conditions where only data from a single curve were available. The results are plotted in Fig. 2.

Adding salt gave rise to an apparent increase of the amount of associated peptide at a given aqueous concentration (except for the range of very low c). At 0.22 M NaCl (where aqueous melittin is still monomeric), a value of $F_\infty = 21\,3000$ ($\pm 3\%$) deg · cm^2 · dmol^{-1} could be evaluated from the data for two values of c_P (5 and 10 μM). The resulting r values as a function of c are also presented in Fig. 2. In addition, there are a few points obtained with 0.1 M NaCl ($F_\infty = 20\,500$ deg · cm^2 · dmol; $c_P = 5$ and 10 μM).

Fluorescence energy transfer

We modified Trp by 2-hydroxy-5-nitrobenzyl bromide so that a non-fluorescent melittin species was formed. This A-melittin can function as an acceptor of fluorescence energy from the Trp in the unmodified peptide, D-melittin. Both melittin species have been shown to be equivalent as far as the formation of tetramers in aqueous solution is concerned [13]. We could verify this with our material. In order to achieve a sufficient overlap of the absorption spectrum of the acceptor with the fluorescence spectrum of the donor, a pH of 5 had to be chosen. Under these conditions, the pertinent spectral overlap integral [17] becomes $J = 2.16 \cdot 10^{-14}$ cm^3 · M^{-1} in the lipid-associated state (Vogel, H., personal communication). The distance of 50% energy transfer between donor and acceptor groups may be calculated according to standard rules [13], resulting in $R_0 = 32.5$ Å.

We have prepared a solution of 10 μM (normal) D-melittin together with vesicles formed of 2 mM DOPC. Then there is practically full association according to the circular-dichroism data. When (modified) A-melittin is added, we observe substantial energy transfer as shown in Fig. 3. Such an effect should be expected, even if no aggregation of the associated peptide occurs. The density of monomers on the vesicle surface would be large enough to reduce the distances between donor and acceptor so that energy transfer can actually take place. The problem has been dealt with in detail by Fung and Stryer [18]. Adopting their theoretical approach, we can fit our data excellently with $R_0 = 33$ Å (see Fig. 3a) assuming association with the outer leaflet of the bilayer, which comprises half of the total lipid (see Discussion). This result agrees very well with our calculated R_0. No significant change could be observed by varying the NaCl concentration from 0 to 1 M (see Fig. 3b).

Kinetic experiments

We have attempted to measure the rate of association in a stopped-flow apparatus. It appeared that the inherent fluorescence change of the Trp group could not be used as a monitoring signal. In order to avoid interference with scattered light in the excitation range (280–290 nm), emission below about 335 nm had to be cut off. Above that wavelength, however, the overall fluorescence of the aqueous and associated peptide is almost the same. Therefore, we employed a more suitable method involving PBA. This substance incorporates into the bilayer and absorbs light in the emission range of the lipid-associated melittin. The latter can accordingly transfer energy to PBA, which then exhibits enhanced fluorescence in the range above 370 nm (see Fig. 4).

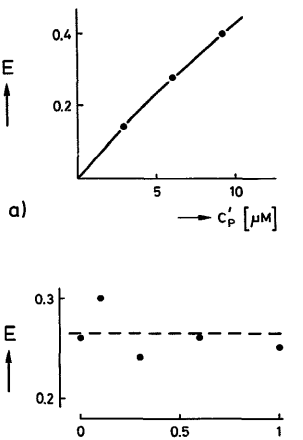

Fig. 3. Energy-transfer efficiency, E, of vesicle-associated melittin (10 μM normal D-melittin/2 mM DOPC) plotted vs. (a) c'_P, the concentration of added modified A-melittin (in the absence of extra salt), where the solid curve is calculated adopting the theory of Fung and Stryer (see text) with $R_0 = 33$ Å and a minimum approach distance of 10 Å, which is, however, not critical [18] and (b) the concentration of added NaCl ($c'_P = 6$ μM).

In our experimental work, rapid mixing has been carried out with aqueous melittin and a vesicle preparation including 1 PBA molecule per 200 lipid molecules. A filter was used to measure the fluorescence intensity above 360 nm. This provided a good signal to follow the association reaction.

In the presence of 0.1 M NaCl, the time-course of the fluorescence change could be well fitted by a single exponential function (see Fig. 5a). The relaxation time,

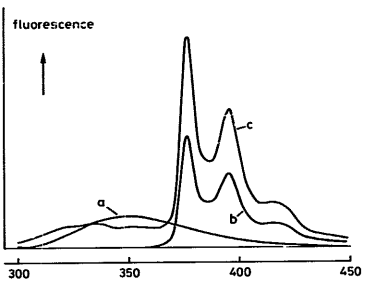

Fig. 4. Fluorescence emission (arbitrary units, excitation at 285 nm, standard buffer) of 10 μM aqueous melittin (a), 5 μM PBA in 1 mM DOPC vesicles (b) and 10 μM melittin added to 5 μM PBA in 1 mM DOPC vesicles (c).

τ, was found to be independent of c_P but decreased at increasing c_L, according to the linear relation

$$1/\tau = k_{as} \cdot c_L + k_{dis} \tag{3}$$

(see Fig. 5b). This is consistent with the basic phenomenological rate scheme

$$P_f + L \underset{k_{dis}}{\overset{k_{as}}{\rightleftharpoons}} P_{as} \tag{4}$$

(P_f, free peptide; L, lipid; P_{as}, lipid-associated peptide) formally described in terms of the appropriate rate constants k_{as} (second order) for the association and k_{dis} (first order) for the dissociation [10]. In a given experiment, c_L remains constant so that the association is actually a pseudo-first-order reaction. We note that the equilibrium condition implies

$$k_{as}/k_{dis} = \bar{r}/\bar{c}_f = \Gamma_{app} \tag{5}$$

where the bars indicate the appropriate equilibrium values and Γ_{app} is the apparent partition coefficient.

From the data of Fig. 5b we obtain

$$k_{as} = 1.4 \cdot 10^5\ M^{-1} \cdot s^{-1} \text{ and } k_{dis} = 14\ s^{-1}$$

This implies an average life-time of the associated state of 70 ms ($= 1/k_{dis}$). However, k_{dis} (being the intercept on the $1/\tau$ axis) appears to be less certain than k_{as} (i.e., the slope of $1/\tau$ vs. c_L). Applying Eqn. 5, one finds $k_{dis} = 9\ s^{-1}$ based on $\Gamma_{app} \approx 1.6 \cdot 10^4\ M^{-1}$, which is evaluated from the association isotherm of Fig. 2 (c_f values are between 0.3 and 0.7 μM, whereas the final degrees of association lie in the range from 90 to 96%).

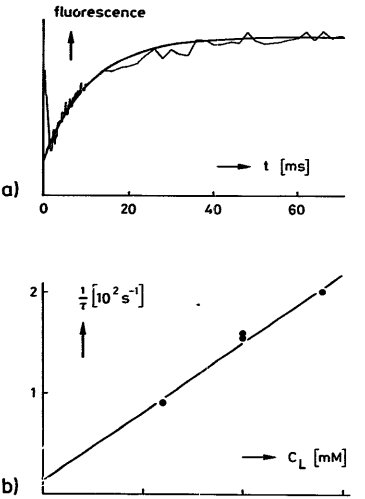

Fig. 5. (a) Fluorescence increase after rapid mixing of melittin with DOPC vesicles (holding 1:200 PBA per lipid) for $c_P = 6$ μM, $c_L = 0.6$ mM in 0.1 M NaCl and standard buffer. The record is fitted by an exponential time function with a relaxation time $\tau = 11$ ms. (b) Plot of reciprocal relaxation times vs. lipid concentration (0.1 M NaCl; $c_P = 6$ M at $c_L = 0.6$ and 1.0 mM, $c_P = 10$ μM at $c_L = 1.0$ and 1.4 mM). It should be emphasized that, under the given conditions, practically no PBA is in the aqueous medium. Therefore, our fluorescence records certainly do not involve appreciable contributions of PBA exchange (this was also directly checked by experiments without melittin) or possibly of melittin-PBA binding. In addition, we note that any of these reaction types is expected to exhibit a concentration-dependence contrary to the one actually observed.

Analogous experiments without added salt exhibited a more complicated picture. Only for a comparatively low melittin concentration could a single exponential time function be recorded. This was the case, for instance, with $c_P = 4$ μM and $c_L = 0.9$ mM, where a $\tau = 9.5$ ms has been determined. For larger c_P, such as 10 and 13 μM (at the same c_L), the rate curves were found to slow down appreciably in the course of the association process. We attribute this to the build-up of electrostatic repulsion by the charges of already associated peptide. In fact, the initial part of the rate curves can be fitted by exponential functions of nearly the same relaxation times, $\tau \approx 8.5\ (\pm 1.0)$ ms (as long as c_L is not changed). This is equivalent to a rate constant of $k_{as} \approx 1.2\ (\pm 0.2) \cdot 10^5\ M^{-1} \cdot s^{-1}$, under conditions where

the repulsive interactions are negligible (calculated on the basis of Eqns. 3 and 5 with $\Gamma_{app} \approx 10^4\ M^{-1}$ as gathered from the appropriate equilibrium data of Fig. 2).

We may conclude that electrostatic interactions influence more intensely the dissociation rate than the rate of association. The present kinetic results seem to suggest an intrinsic association rate constant of approx. $1.3 \cdot 10^5\ M^{-1} \cdot s^{-1}$, which is little affected by the electrolyte concentration or the peptide-to-lipid ratio. The observed changes of Γ_{app} would therefore reflect effects on k_{dis}. More quantitatively, the mean life-time of the associated peptide amounts to about 100 ms at lower r (about 0.01) and tends to decrease at higher peptide-to-lipid ratios, presumably due to electrostatic repulsion of neighboring peptide molecules. This tendency can be moderated by adding an electrolyte.

Discussion

We recall that no special molecular model has been assumed in order to evaluate from the measured results the data points of Fig. 2. For a quantitative interpretation, however, one must introduce a basic idea of the nature of the underlying association process. It appears most appropriate to choose a partitioning approach which implies the peptide becomes 'dissolved' in the lipid bilayer due to favorable solvation effects exerted by the lipid.

The unilamellar vesicles prepared in the present work are fairly small, having an approximate diameter of 300 Å [9]. Accordingly, we estimate that some 60% of the lipid is concentrated in the outer leaflet of the bilayer, to which initially the peptide can associate. However, the interaction with melittin is known to transform small vesicles into much larger ones (more than 1300 Å diameter) [6,19,20]. Nevertheless, association still occurs only on the outer surface of the bilayer [4,13,21]. Therefore, an outer leaflet including only about 50% of the total lipid is considered in the discussion of our equilibrium studies.

The partition equilibrium

Let us envisage purely monomeric melittin in the aqueous as well as in the bilayer phase. The partition equilibrium is then described by

$$r = (\Gamma_1/\alpha_1) \cdot c_f \qquad (6)$$

involving a (concentration-independent) partition coefficient, Γ_1, which is determined by the free-energy difference of the substrate between the two media, and an activity coefficient α_1, which reflects possible non-ideal solute–solute interactions (defined so that $\alpha_1 \to 1$ at $r \to 0$). This can be generally derived from thermodynamic principles [8] (see also Appendix).

In the case of negligible solute–solute interactions, where $\alpha_1 = 1$, Eqn. 6 predicts the association isotherm to be a straight line through the origin. The fact that we observe a pronounced curvature with gradually decreasing values of $\Gamma_{app} = r/c_f$ suggests the existence of repulsive interactions between the associated peptide monomers (attractive forces in the aqueous phase could actually cause the same effect, but this is disregarded here because of the very low c). We attribute these interactions primarily to electrostatic repulsions of the positively charged melittin molecules. Their average distances on the water/lipid interface indeed become sufficiently reduced when compared with the aqueous solution state. Taking advantage of the Gouy-Chapman model approach for charged surfaces, the appropriate activity coefficient is found to be expressed according to

$$\ln \alpha_1 = 2\nu \cdot \sinh^{-1}(\nu b r) \qquad (7)$$

where the parameter ν stands for the effective number of charges per peptide chain and b is a dimensionless quantity depending on the salt content in the aqueous phase. A detailed discussion is given in the Appendix.

Under our present experimental conditions, we obtain $b = 38.9$ (no NaCl), 11.5 (0.1 M NaCl) and 8.1 (0.22 M NaCl) by application of Eqn. A5c (with $A_L = 0.70\ nm^2$ [9], $\beta = 0.5$, $\epsilon = 81$ and a contribution of buffer to the total salt taken as 0.01 M). Then Eqn. 6 involves only two adjustable parameters, Γ_1 and ν, in order to attempt a fit of our data. Such fits can indeed be very well achieved, as demonstrated in Fig. 2, where the appropriate values of Γ_1 and ν are given in the legend.

The apparent value of ν of around 2 turns out to be substantially smaller than that value between 5 and 6 which is expected for the actual charge of a melittin molecule at the given pH. A similar discrepancy has been observed before and can be readily attributed to the existence of discrete charges in contrast to the assumption of a continuous charge-density in the Gouy-Chapman model [22]. Another contribution towards that reduced ν could result from a partial neutralization by counterions (see Appendix). The obvious decrease of the partition coefficient at higher ionic strength is easily explained on the basis of an enhanced solubility of the highly charged peptide in the aqueous phase, due to the favorable effect of ionic-cloud formation.

The question of melittin aggregation in the bilayer

We have investigated in some detail a possible tetramerization process. In such a case, one obtains the following relations (see Appendix, Eqn. A11)

$$r = r_1 \cdot \left[1 + (2r_1/r^*)^3\right] \quad \text{with } r_1 = (\Gamma_1/\alpha_1) \cdot c_f$$

where α_1 is determined by the total r as specified by Eqn. 7 and r^* stands for the critical value of r corresponding to 50% aggregation. Recalling the curves in Fig. 2, we note that $r^* \geq 0.1$ implies that practically no aggregation occurs within our range of concentrations. Then, for instance, the 0.22 M salt data are fitted with $\nu = 2.05$ and $\Gamma_1 = 3.2 \cdot 10^4\ M^{-1}$. However, if we arbitrarily set $r^* = 0.02$ (equivalent to a pronounced degree of tetramerization), an equally good fit can be obtained just by raising ν from 2.05 to 2.5 without changing Γ_1.

Actually all our present data are found to be compatible with any chosen tendency of tetramerization, if only the parameters ν and Γ_1 are properly adjusted. Therefore, the measured association isotherms do not rule out the possibility of aggregation of the membrane-associated peptide. Nevertheless, evidence that, in fact, no such aggregation occurs can be gathered from our fluorescence energy transfer experiments. They have merely shown the effect of associated monomers. Although these experiments were carried out at pH 5, we expect no essentially different situation at our otherwise higher pH of 7, at which value the repulsive charges are largely retained. Indeed, lack of aggregation in the bilayer is supported by recent reports [23–25] as far as the conditions (approx. 0.2 M NaCl or less, pH 7) in the present partitioning and kinetic studies are concerned.

Kinetics of the partitioning

We note that the phenomenological rate scheme 4 may be resolved as

$$P_f + L \underset{k_{-d}}{\overset{k_d}{\rightleftharpoons}} P_{enc} \underset{k_{-c}}{\overset{k_c}{\rightleftharpoons}} P_{as} \qquad (8)$$

where P_{enc} denotes the intermediate steady-state encounter complex, i.e., the peptide in the (disordered) P_f conformation when it touches the bilayer surface. The rate constants k_d and k_{-d} are controlled by diffusion in the aqueous medium. k_c and k_{-c} then describe the forward and reverse rates of converting P_{enc} to the final P_{as}, involving incorporation in the bilayer and a simultaneous change of conformation. Based on the detailed treatment of this problem given elsewhere [10,26], we calculate for the present system

$$k_d \approx 4.2 \cdot 10^6\ M^{-1} \cdot s^{-1} \quad \text{and} \quad k_{-d} \approx 8.3 \cdot 10^6\ s^{-1}$$

using an aqueous diffusion coefficient $D_0 \approx 2.5 \cdot 10^{-6}\ cm^2 \cdot s^{-1}$ [15] and a corresponding Stokes radius $R_0 \approx 10$ Å. In view of the theoretical relation A14a, our experimental k_{as} then results in $k_c \approx 3 \cdot 10^5\ s^{-1}$.

A more detailed analysis of the conversion $P_{enc} \rightarrow P_{as}$ (see Appendix) yields the expression A16, namely

$$k_c = [q\gamma' k_s / (q\gamma' k_s + k_t)] \cdot k_t$$

where k_t stands for the diffusion-controlled rate constant of the P_f conformation penetrating the bilayer, k_s is the rate constant of the conformational transition ($P_f \rightarrow P_{as}$) in the membrane associated state, γ' denotes the ordinary partition coefficient (molar concentration basis) of the structurally unchanged P_f form and $q = d/2R_0$ (d is the thickness of the bilayer) is the volume ratio of the bilayer and encounter spaces. Following previous reasoning [10], we estimate $k \geq 10^7\ s^{-1}$. Thus, in view of the above experimental value of k_c, the structural transition upon melittin association appears to be rate-determining, so that Eqn. 14 becomes

$$k_c = q\gamma' k_s$$

The value of γ' is not known. At any rate, however, it should be much smaller than the experimental partition coefficient which includes the conformational transition to the final P_{as} state, i.e., $\gamma' \ll \gamma = \Gamma_1 / V_L$ ($V_L \approx 0.8\ dm^3 \cdot mol^{-1}$ [9] being the partial molar volume of the lipid). This implies $k_s \lesssim 10^2\ s^{-1}$, which appears to be a reasonable rate constant for a membrane-associated change of secondary structure. It is of the same order of magnitude as found recently with alamethicin [10].

So far, these considerations have disregarded electrostatic repulsion effects due to the accumulation of positive charge in the course of the association reaction. As has been observed in our experiments, such repulsion is negligible at higher salt concentrations, or below a certain concentration of associated peptide. Under other conditions, a pronounced slowing down of the reaction occurs. In order to describe this quantitatively, a more sophisticated theoretical approach is needed, which will not be attempted in the present article.

Acknowledgements

This work was supported by Grant No. 3.285.85 from the Swiss National Science Foundation. We are grateful to Dr. H. Vogel for helpful discussions and advice.

Appendix

Chemical potentials of associated molecules

Let us assume that a substrate can associate with an electrically neutral lipid bilayer as aggregates of any number, i, of charged monomers. In the first step, we consider the association when there is no charge on these monomers. The Gibbs free energy of the bilayer phase as a whole may then be written

$$G' = n_L \cdot \mu'_L + \Sigma_i n_i \cdot \mu'_i \qquad (A1)$$

where μ'_L and μ'_i stand for the appropriate chemical potentials of the lipid and individual associated aggre-

gates, respectively (n_L and n_i denote the mole numbers). In the second step, the charge is imagined to be added gradually. This requires an amount of work, w. The final free energy of the charged system becomes $G = G' + w$. Accordingly, the chemical potential of the charged aggregate state, i, can be derived as

$$\mu_i = \mu_i' + (\partial w/\partial n_i) \tag{A2}$$

holding constant p, T and all mole numbers except n_i.

Basically, we have

$$w = \int_0^{Q} \phi(Q)\,\mathrm{d}Q \tag{A3}$$

involving the electric potential ϕ on the bilayer surface when the total charge is Q. The final charge will be

$$Q_0 = \nu e_0 \cdot N_A \cdot r \cdot n_L \tag{A4}$$

with ν being the number of charges per monomer (e_0 is the elementary charge, N_A is Avogadro's number). On the condition that Q is uniformly distributed over the interface between the outer leaflet of the bilayer and the electrolyte, we can express $\phi(Q)$ by applying the Gouy-Chapman model theory [27]. This eventually results in

$$w = (N_A e_0 n_L/b) \cdot \int_0^{\nu br} \psi(y)\,\mathrm{d}y \tag{A5a}$$

$$\psi(y) = (2kT/ze_0) \cdot \sinh^{-1}(\nu br) \tag{A5b}$$

$$b = (e_0/A_L \cdot \beta) \cdot (8\epsilon_s \epsilon RTc_s)^{-1/2} \tag{A5c}$$

provided the electrolyte is a salt which dissociates completely in z-valent ions (c_s is the concentration of salt, A_L the area per lipid on the outer surface, β the fraction of lipid making up the outer leaflet, k is Boltzmann's constant, T the absolute temperature, R the gas constant, ϵ_s the permittivity of vacuum and ϵ the dielectric constant of the aqueous phase).

At a lower degree of association, effects other than electrostatic may be disregarded, so that

$$\mu_i' = \mu_i^{\theta} + RT \cdot \ln r_i \tag{A6}$$

($r_i = n_i/n_L$) with an appropriate standard chemical potential, μ_i^{θ} [8]. Recalling the Eqns. A2 and A5 we then obtain

$$\mu_i = \mu_i^{\theta} + RT \ln(\alpha_i \cdot r_i) \tag{A7a}$$

where

$$\alpha_i = \exp[(2i/z) \cdot \nu \cdot \sinh^{-1}(\nu br)] \tag{A7b}$$

is the adequate activity coefficient describing non-ideality due to electrostatic repulsions between aggregates.

It must be emphasized that the present approach suffers from certain shortcomings. These imply appreciably too large values of $\phi(Q)$ and therefore also of α_i if ν_0, the actual number of charges per monomer on the associated substrate, is considered when specifying the theoretical parameter, ν. One serious point concerns the premise of a continuous charge-distribution in the interface between the lipid and aqueous phases. In reality, we deal, however, with a distribution of discrete charges which, in addition, may even be located some distance from the interface. This discrete charge effect alone could cause a substantial reduction of the apparent value of ν compared with ν_0 [22]. Another point to be taken into account arises from the fact that, in practice, the associated substrate cannot be charged without also introducing, the countercharges. Depending on their final mean distance from the bilayer (relative to the extension of the ionic atmosphere), the effective work will so be smaller than that calculated above. This countercharge effect is equivalent to a partial neutralization of substrate charge.

Association isotherms

The partitioning of charged substrate between an aqueous phase and the bilayer may be described analogously as pointed out in some detail previously with the uncharged peptide alamethicin [8,9]. The free (i.e., non-associated) aqueous state of the substrate is supposed to be purely monomeric and sufficiently dilute so that its chemical potential can be written in the ideal form

$$\mu_f = \mu_f^{\infty} + RT \cdot \ln c_f \tag{A8}$$

(μ_f^{∞} being the standard value related to infinite dilution). Under equilibrium conditions, this must be equal to μ_1, the chemical potential of bilayer-associated monomers (see Eqn. A7 for $i = 1$). Accordingly, we derive the relation

$$r_1 = (\Gamma_1/\alpha_1) \cdot c_f \tag{A9a}$$

which involves the partition coefficient of monomers, namely

$$\Gamma_1 = \exp(-\Delta\mu_1^{\theta}/RT) \tag{A9b}$$

as determined by the difference of standard free energies, $\Delta\mu_1^{\theta} = \mu_1^{\theta} - \mu_f^{\infty}$, between the two media.

Not all of the associated substrate may exist as monomers, owing to aggregation. For the sake of simplicity, we shall discuss here only the possible case of tetramerization (in the bilayer phase). The mass-action law apparently reads

$$r_4 = K_4 \cdot (\alpha_1 r_1)^4/\alpha_4 = K_c \cdot r_1^4 \tag{A10}$$

(K_4 is the thermodynamic equilibrium constant; note

that Eqn. A7b implies $\alpha_4 = \alpha_4^4$). Having defined a critical value $r^* = (2/K_4)^{1/3}$, the total associated substrate-to-lipid ratio becomes

$$r = r_1 + 4r_4 = r_1 \cdot [1 + (2r_1/r^*)^3] \tag{A11}$$

At $r = r^*$, just 50% of the available substrate is aggregated (i.e., $4r_4/r = 0.5$).

Provided the aggregation parameter r^* is given, the association isotherm may be calculated as follows. Starting from a certain r, the value of r_1 is evaluated by means of Eqn. A11. Then, because of Eqns. A9 and A7b, we have

$$c_f = (r_1/\Gamma_1) \cdot \exp[2\nu \sinh^{-1}(\nu br)] \tag{A12}$$

where Γ_1 and ν are adjustable in order to fit experimental data (b is fixed by known properties of the system, see Eqn. A5c).

Anatomy of the association rate constant

Basically, the mechanism of association may be described as a series of three steps, two being controlled by diffusion (in the aqueous and bilayer media) and a third which comprises the inherent transition of secondary structure. We represent this by the scheme

$$P_f + L \underset{k_{-d}}{\overset{k_d}{\rightleftharpoons}} P_{enc} \underset{k_{-t}}{\overset{k_t}{\rightleftharpoons}} P'_{as} \underset{k_{-s}}{\overset{k_s}{\rightleftharpoons}} P_{as} \tag{A13}$$

as already introduced above. A detailed and rather general discussion can be found elsewhere [10,25]. Here we shall give only a brief comment on the approach to express the phenomenological rate constant k_{as} in terms of the intermediate rate constants of scheme A13.

The states P_{enc} and P'_{as} refer to the substrate molecule in the P_f conformation when it has reached a position on the bilayer surface or at the site of association, respectively. Both states can be assumed to have a population much smaller than that of P_f and/or P_{as}. Therefore, those intermediate states must be subject to steady-state equilibria, implying that the overall reaction $P_f + L \rightarrow P_{as}$ can be described by a second-order rate constant

$$k_{as} = [k_c/(k_{-d} + k_c)] \cdot k_d \tag{A14a}$$

involving a first-order rate constant

$$k_c = [k_s/(k_{-t} + k_s)] \cdot k_t \tag{A14b}$$

which applies to the conversion $P_{enc} \rightarrow P_{as}$. We prefer, however, to eliminate explicit use of k_{-t}, taking advantage of the relation

$$k_t/k_{-t} = n_{as}/n_{enc} = q\gamma' \tag{A15}$$

where n_{as} and n_{enc} stand for the respective mole numbers under equilibrium conditions. The ordinary partition coefficient (volume concentration basis) of the structurally unchanged substrate is denoted γ', whereas q is the ratio of the volumes available for the associated and encounter states. The value of γ' is determined by the free-energy difference of the P_f conformation between the bilayer and aqueous media. Naturally, we except that γ' is much less than γ, the value applicable to the final P_{as} conformation.

Considering $q\gamma' k_{-t} = k_s$, Eqn. A14b then becomes

$$k_c = [q\gamma' k_s/(q\gamma' k_s + k_s)] \cdot k_t \tag{A16}$$

In the case where the whole bilayer volume is accessible to the associated substrate, $q \approx d/2R_0$ (d is the thickness of the bilayer, $2R_0$ the effective diameter of the substrate molecule in its aqueous form). Note that previously, [10], the factor q was inadvertently omitted. Such omission does, however, not cause serious harm, since q is usually a number close to unity.

References

1 Habermann, E. (1972) Science 177, 314–321.
2 Knöppel, E., Eisenberg, D. and Wickner, W. (1979) Biochemistry 18, 4177–4181.
3 Vogel, H. (1987) Biochemistry 26, 4562–4572.
4 Stanislawski, B. and Rüterjans, H. (1987) Eur. Biophys. J. 15, 1–12.
5 Tosteson, M.T. and Tosteson, D.C. (1981) Biophys. J. 36, 109–116.
6 Dufourcq, E.J., Smith, E.C.P. and Dufourcq, J. (1986) Biochemistry 25, 6448–6455.
7 Sessa, G., Freer, J.H., Colacicco, G. and Weissman, G. (1969) J. Biol. Chem. 244, 3575–3582.
8 Schwarz, G., Stankowski, S. and Rizzo, V. (1986) Biochim. Biophys. Acta 861, 141–151.
9 Rizzo, V., Stankowski, S. and Schwarz, G. (1987) Biochemistry 26, 2751–2759.
10 Schwarz, G., Gerke, H., Rizzo, V. and Stankowski, S. (1987) Biophys. J. 52, 685–692.
11 Shipolini, R.A., Gallewaert, G.L., Cottrell, R.C., Doonan, S., Vernon, C.A. and Banks, B.E.C. (1971) Eur. J. Biochem. 20, 459–468.
12 Quay, S.C. and Condie, C.C. (1983) Biochemistry 22, 695–700.
13 Vogel, H. and Jähnig, F. (1986) Biophys. J. 50, 573–582.
14 Paul, C., Kirschner, K. and Haenisch, G. (1980) Anal. Biochem. 101, 442–448.
15 Podo, F., Strom, R., Crifo, C. and Zulauf, M. (1982) Int. J. Pept. Prot. Res. 19, 514–527.
16 Vogel, H. (1981) FEBS Lett. 134, 37–42.
17 Förster, Th. (1948) Ann. Physik 2, 55–75.
18 Fung, B.K. and Stryer, L. (1978) Biochemistry 17, 5241–5248.
19 Morgan, C.G., Williamson, H., Fuller, S. and Hudson, B. (1983) Biochim. Biophys. Acta 732, 668–674.
20 Dufourcq, J., Faucon, J., Fourche, G. Dasseux, J., Maire, M. and Gilik-Krzywicki, T. (1986) Biochim. Biophys. Acta 859, 33–48.
21 Strom, R., Podo, F., Crifo, C., Berthet, C., Zulauf, M. and Zaccai, G. (1983) Biopolymers 22, 391–397.
22 Schoch, P. and Sargent, D.F. (1980) Biochim. Biophys. Acta 602, 234–247.
23 Hermetter, A. and Lakowicz, J.R. (1986) J. Biol. Chem. 261, 8243–8248.
24 Talbot, J.C., Faucon, J.F. and Dufourcq, J. (1987) Eur. Biophys. J. 15, 147–157.
25 Altenbach, C. and Hubbel, W.L. (1988) Proteins 3, 230–242.
26 Schwarz, G. (1987) Biophys. Chem. 26, 163–169.
27 Hiemenz, P.C. (1986) Principles of Colloid and Surface Chemistry, pp. 697–703, Marcel Dekker, New York.